

A QUANTITATIVE STUDY OF INTERACTING DARK MATTER IN HALOS

C.S. KOCHANEK AND MARTIN WHITE

Harvard-Smithsonian Center for Astrophysics, Cambridge, MA 02138

ckochanek, mwhite@cfa.harvard.edu

Draft version November 10, 2018

ABSTRACT

We study the evolution of Hernquist profile “galaxies” in the presence of self-interacting dark matter (SIDM), where the properties of the dark matter can be parameterized by one number, $\hat{\sigma}_{DM} = \sigma_{DM} M_T / a^2$ for a halo of mass M_T and break radius a . While the halos form constant density cores of size $\sim a/2$ on the core radius relaxation time scale ($t_{rc} \simeq 1.7 t_{\text{dyn}} / \hat{\sigma}_{DM}$) core collapse begins shortly thereafter and a steeper $1/r^2$ central density cusp starts forming faster than predicted by 2-body relaxation. The formation of the steeper central cusp is accelerated if the cooling baryons adiabatically compress the dark matter. The natural consequence of SIDM is to exacerbate rather than to mitigate astrophysical problems created by dark matter density cusps.

Subject headings: cosmology:theory – galaxies:formation – methods:numerical – dark matter

1. INTRODUCTION

A model based on the growth of small fluctuations through gravitational instability in a universe with cold dark matter (CDM) provides an excellent fit to a wide range of observations on large scales ($\gg 1\text{Mpc}$). However the nature and properties of the CDM, apart from its being cold and dark, remain mysterious. It is one of the major goals of cosmology to further constrain the properties of the dark matter and determine its nature. Recently much attention has been refocused on this question because of a suggestion by Spergel & Steinhardt (2000) that possible discrepancies with observations on kpc scales could be probes of dark matter properties, particularly its self-interaction rate. In its simplest incarnation, the self-interacting dark matter (SIDM) model provides a 1-parameter family of models with standard CDM as a limiting case, and it is thus interesting to examine this model in some detail.

In this paper we calculate the quantitative effects of SIDM on the evolution of isolated halos using an N-body code with particle scattering. We review the astrophysical arguments motivating SIDM in §2 and describe our implementation of the scattering algorithm in §3 (our method is very similar to that of Burkert (2000), but uses a more accurate approximation to the scattering rate integral). The impact of self-interaction on various astrophysical processes is discussed in §4 and we finish with some conclusions in §5.

2. THE CASE FOR SIDM

In this section we briefly recap the arguments which led Spergel & Steinhardt (2000) to revive the SIDM model (Carlson et al. 1994; de Laix, Scherrer & Schaeffer 1995) since it is precisely these astrophysical observations that can be used to constrain the self-interaction of dark matter.

There is a growing consensus that CDM halos form with central density cusps, where $\rho \sim r^{-\gamma}$ as $r \rightarrow 0$ with $\gamma \simeq 1$ (Navarro et al. 1997; Moore et al. 1998; Huss et al. 1999; Klypin et al. 1999; Moore et al. 2000a; but see Kravstov et al. 1998). Analytic arguments (Syer & White 1998;

Kull 1999) suggest that such a core structure follows naturally from merging in collisionless systems. These results are (in some senses) confirmed experimentally by the similar stellar density cusps found in early-type galaxies (e.g. Faber et al. 1997), which also largely formed through the merging of collisionless matter (stars). However, such density cusps are inconsistent with the finite core radius required to reproduce the rotation curves of dwarf galaxies (Moore 1994; Flores & Primack 1994). The problem appears to be limited to very low rotation speed galaxies ($v_c < 10^2 \text{ km s}^{-1}$) as van den Bosch et al. (2000) have now shown that the slightly more massive LSBs (low surface brightness galaxies) actually *require* cusped dark matter profiles. CDM simulations also produce halos which correctly reproduce the numbers of galaxies in clusters, but at first sight grossly overpredict the number of satellites orbiting the Galaxy (Moore et al. 1999).

One solution to the discrepancies is to blame the differences on the effects of the baryons. The dwarf galaxies are the systems where the baryons can most easily modify the core structure of the dark matter (e.g. Hernquist & Weinberg 1992; Navarro Eke & Frenk 1996; Gelato & Sommer-Larsen 1999; Binney, Gerhard & Silk 2000) although it is difficult to quantitatively estimate the effects of feedback (e.g. MacLow & Ferrara 1999). Similarly, massive spiral galaxies are probably the best environment for the effects of the baryons to modify the satellite predictions of pure dark matter simulations (e.g. Bullock, Kravstov & Weinberg 2000). It is, however, unclear whether the baryons can provide a complete solution to the two problems. A second solution is to use hot rather than cold initial conditions for the collapsing dark matter (e.g. Hozumi, Burkert & Fujiwara 2000).

Self-interacting dark matter may be a third solution, because it can also heat the cores of dark matter halos and evaporate orbiting satellites given an appropriately tuned interaction cross section. This idea has attracted considerable attention (Ostriker 2000; Hannestad 2000; Hogan & Dalcanton 2000; Burkert 2000; Firmani et al. 2000; Mo & Mao 2000; Hannestad & Scherrer 2000, Bento et al. 2000), but the detailed quantitative consequences of the theory have yet to be derived. We have used N-body methods,

discussed in the next section, to explore the formation and evolution of “galaxies” in a simple model.

3. NUMERICAL METHODS

Throughout we shall study 10^5 particle realizations of a Hernquist profile (Hernquist 1990)

$$\rho_H(r) = \frac{M_T a}{2\pi r} \frac{1}{(r+a)^3} \quad (1)$$

which has two parameters: the total mass M_T and break radius a . The orbital time at the break radius a is $t_{\text{dyn}} = 4\pi(a^3/GM_T)^{1/2}$, which we shall sometimes refer to as the “dynamical time”. With 10^5 particles we can probe the halo structure down to $\sim 0.1a$, which is sufficient for our purposes. We evolve the system using a *Tree* code described in Appendix A.

In addition to the usual gravitational force, we implement the self-interaction of the dark matter using a Monte-Carlo technique. First let us define some dimensionless units. For a galaxy of mass M_0 and radius R_0 (where $M_0 = M_T$ and $R_0 = a$ for the Hernquist model) define a density scale $\rho_0 = M_0/R_0^3$, a velocity scale $v_0 = (GM_0/R_0)^{1/2}$ and a time scale $t_0 = R_0/v_0$. The simplest self-interaction has the scattering cross section per unit mass of the dark matter, σ_{DM} , independent of energy. In this case we obtain the 1-parameter family of models which we shall study here. The scattering rate for a particle with velocity \mathbf{v}_0 is

$$\Gamma = \frac{dn}{dt} = \int d^3\mathbf{v}_1 f(\mathbf{v}_1) \rho \sigma_{DM} |\mathbf{v}_0 - \mathbf{v}_1| \quad (2)$$

where $f(\mathbf{v}_1)$ is the local distribution function of velocities. In dimensionless units,

$$\hat{\Gamma} = \frac{dn}{dt} = \hat{\sigma}_{DM} \int d^3\hat{\mathbf{v}}_1 f(\hat{\mathbf{v}}_1) \hat{\rho} |\hat{\mathbf{v}}_0 - \hat{\mathbf{v}}_1| \quad (3)$$

with dimensionless cross section $\hat{\sigma}_{DM} = M_0 \sigma_{DM} / R_0^2$. For a Hernquist model the fraction of the particles interacting per crossing time t_0 is $0.05\hat{\sigma}_{DM}$, the mean free path is $a/\hat{\rho}\hat{\sigma}_{DM}$, and these interactions have a typical radius $\sim a/2$. We shall quantify the effect of self-interaction as a function of $\hat{\sigma}_{DM}$, and one can then scale to cases of astrophysical interest by suitable choice of the basic dimensional parameters M_0 and R_0 .

We have simulated dimensionless cross sections of $\hat{\sigma}_{DM} = M_T \sigma_{DM} / a^2 = 0, 0.3, 1.0, 3.0$ and 10.0 . For $\hat{\sigma}_{DM} = 1$ we also ran a case with 8×10^5 particles, doubling the spatial resolution, and a case using the Burkert (2000) scattering algorithm for comparison. The evolution of Navarro, Frenk & White (1997) models should be similar if we scale the two models to have the same central density distribution. For this normalization, the evolution of an NFW model will match that of our Hernquist models if $\hat{\sigma}_{DM} = 2\pi\delta_c\rho_{crit}r_c\sigma_{DM}$.

To implement the scattering in an N-body code we need to discretize the calculation of the integral to compute the scattering rate for each particle. Call the particle whose rate we are calculating 0 and particle j the particle from which it is scattering. We approximate the local density from the total mass and radius enclosed by the $N = 32$ nearest neighbors which we order in increasing distance

from particle 0. Writing the masses and velocities of the neighbors as \hat{m}_j and $\hat{\mathbf{v}}_j$ with $j = 1, \dots, N$ we estimate the scattering rate for particle 0 by

$$\hat{\Gamma} = \hat{\sigma}_{DM} \hat{\rho}_N \frac{\sum_{j=1}^N \hat{m}_j |\mathbf{v}_j - \mathbf{v}_0|}{\sum_{j=1}^N \hat{m}_j} \quad (4)$$

where

$$\hat{\rho}_N = \frac{3 \sum_{j=1}^N \hat{m}_j}{4\pi r_N^3} \quad (5)$$

is the estimate of the local density. Note that this differs from the prescription of Burkert (2000) who simply approximated $|\Delta\mathbf{v}| = |\mathbf{v}_0|$, thereby underestimating the heating rate for low velocity particles.

For time step $\Delta\hat{t}$ the probability of an interaction during the time step is $P_{\text{int}} = \hat{\Gamma}\Delta\hat{t}$. We adjust the time steps to keep the interaction probability relatively low ($P_{\text{int}} < 0.5$), and the actual number of interactions in each time step is determined from the Poisson distribution with an expectation value of P_{int} . For each scattering event we interact with one of the N nearest particles, where the probability of interacting with particle j is

$$p_j = \frac{m_j |\mathbf{v}_j - \mathbf{v}_0|}{\sum_{i=1}^N m_i |\mathbf{v}_i - \mathbf{v}_0|} \quad (6)$$

This makes the interaction less “point-like”, but it provides a more correct estimate of the scattering rates and their dependence on particle energy. We have run one simulation ($\hat{\sigma}_{DM} = 1$) with 8 times as many particles to estimate the systematic error induced by this non-locality, and find that it is negligible (see Fig. 2a).

Once a particle is selected for the interaction, we assume that the scattering is isotropic. For particles with center of mass velocity \mathbf{v}_c and velocity difference $\Delta\mathbf{v}$, we select a random direction \mathbf{e} and assign the particles velocities of

$$\mathbf{v}_0 = \mathbf{v}_c + |\Delta\mathbf{v}| \mathbf{e} m_j / (m_0 + m_j) \quad (7)$$

$$\mathbf{v}_j = \mathbf{v}_c - |\Delta\mathbf{v}| \mathbf{e} m_0 / (m_0 + m_j). \quad (8)$$

Such elastic scattering will conserve energy and linear momentum, but not angular momentum because of the finite particle separations. However, the net violation of angular momentum conservation over all interactions will be zero because the particle separation vectors have random orientations. The finite interaction range also leads to diffusion effects, but these introduce negligible error as we can see by comparing to our higher resolution simulation (Fig. 2a).

Finally we note that several simulations have been run approximating self-interacting dark matter as a fluid and using numerical hydrodynamic techniques (Moore et al. 2000b; Yoshida et al. 2000). This is a physically different regime from the low optical depth system proposed by Spergel & Steinhardt (2000). Unlike a strongly interacting fluid, the energy transfer in SIDM is dominated by stochastic collisions in the core which rapidly transport the energy into the outskirts of the halo. The fluid results are thus not directly applicable. The physical problem SIDM most closely resembles is 2-body relaxation in globular clusters (see Spergel & Steinhardt 2000; Hannestad 2000; Burkert 2000).

4. RESULTS

We considered a series of experiments comparing the evolution of N-body systems with and without SIDM parameterized by $\hat{\sigma}_{DM}$. The key to understanding their evolution is the relaxation time due to the scattering. It is, however, a different regime from normal 2-body relaxation. The scattering process is direct rather than diffusive and the structure of the system evolves on the relaxation time scale rather than on a large multiple of the relaxation time scale as in globular clusters. We first define a relaxation time for SIDM, and then compare the evolution of three dynamical systems with and without SIDM. We begin with the evolution of Hernquist profile galaxies, next we consider the effects of adiabatic compression of the dark matter by the baryons in modifying this evolution, and finally we examine the collapse of a cold top-hat perturbation.

4.1. Relaxation time

For 2-body relaxation, the relaxation time is defined to be $\sigma^2/D(v_{\text{para}}^2)$ where σ is the one-dimensional velocity dispersion and $D(v_{\text{para}}^2)$ is the diffusion coefficient parallel to the particle velocity (see Binney & Tremaine 1987; §8). For SIDM, the scattering angle average of the velocity change is just $\frac{1}{2}|\Delta\mathbf{v}|^2$ so the analogy of the 2-body relaxation diffusion coefficient is

$$D(v^2) = \frac{1}{2} \int \rho \sigma_{DM} |\Delta\mathbf{v}|^2 f(\mathbf{v}_0) f(\mathbf{v}_1) d^3\mathbf{v}_0 d^3\mathbf{v}_1 \quad (9)$$

$$= \frac{16}{\sqrt{\pi}} \rho \sigma_{DM} \sigma^3 \quad (10)$$

assuming that the particle velocity distributions $f(\mathbf{v})$ are Maxwellians with one-dimensional velocity dispersions of σ . The relaxation time is then

$$t_r \equiv \frac{3\sigma^2}{D(v^2)} \simeq \frac{1}{3\rho\sigma_{DM}\sigma} \quad (11)$$

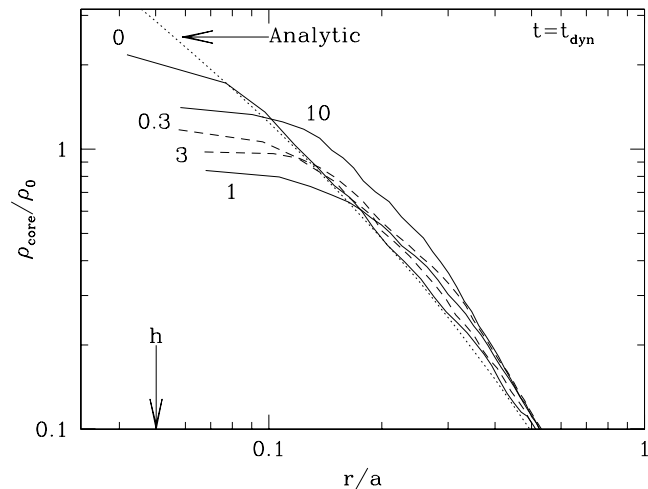


FIG. 1.— (Top) The halo density profiles at $t \simeq t_{\text{dyn}}$ for models with $\hat{\sigma}_{DM} = 0, 0.3, 1.0, 3.0$ and 10.0 . The dotted line shows the initial Hernquist profile. Note that after only one dynamical time the $\hat{\sigma}_{DM} = 3$ and 10 cases have started to core collapse. The force softening is indicated by h .

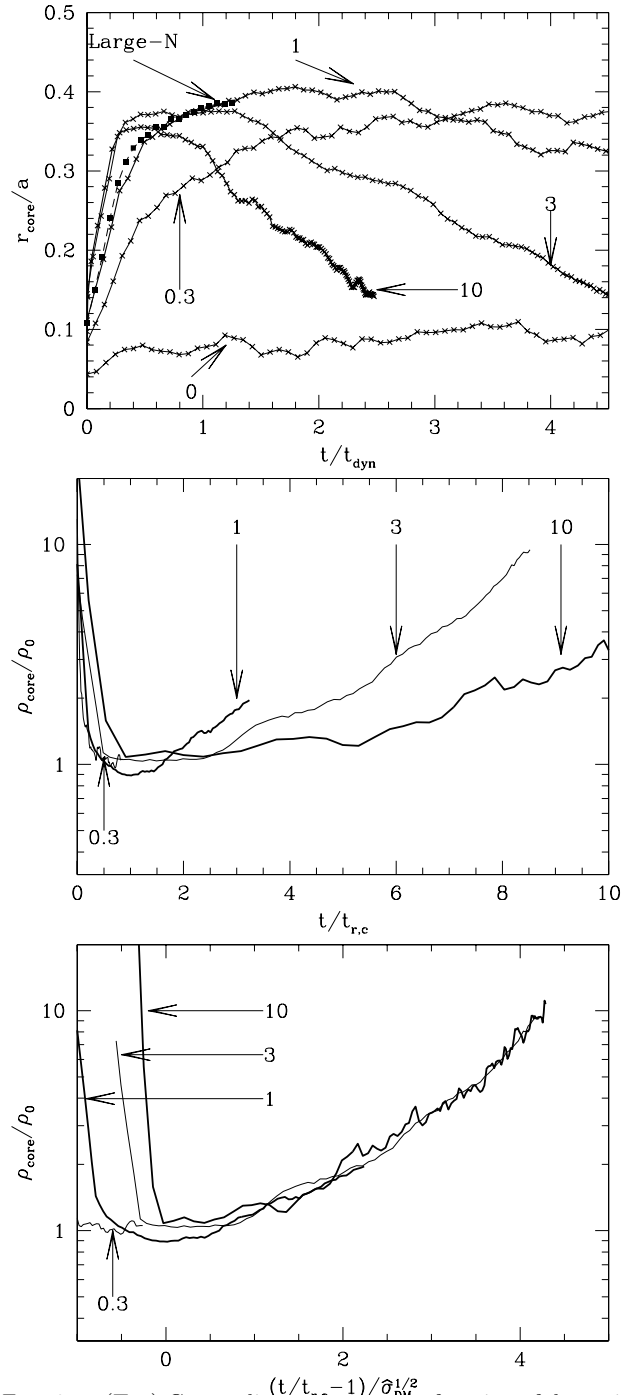


FIG. 2.— (Top) Core radius evolution as a function of dynamical time. The solid lines show the evolution of the core radius (temporally smoothed) for dimensionless cross sections of $\hat{\sigma}_{DM} = 0, 0.3, 1.0, 3.0$ and 10.0 . Note that the standard (10^5 particles) and “Large-N” (8×10^5 particles) simulations for $\hat{\sigma}_{DM} = 1$ show identical evolution. (Middle) Central density evolution as a function of relaxation time $t_{rc} = 1.7t_{\text{dyn}}/\hat{\sigma}_{DM}$. As expected, the minimum core density occurs at $t_{rc} \simeq 1$. (Bottom) Recollapse. The recollapse of the core after reaching maximum expansion near $t/t_{rc} = 1$ is self-similar for a time scale of $t_{rc}\hat{\sigma}_{DM}^{1/2}$.

where the factor of 3 arises because we considered the total velocity rather than a single component. The relaxation time associated with the mean interaction radius $a/2$, which we will call the core relaxation time, is $t_{rc} = 1.7t_{\text{dyn}}/\hat{\sigma}_{DM}$. At the Hernquist break radius the relaxation time is $8t_{\text{dyn}}/\hat{\sigma}_{DM}$ and at the half-mass radius (2.4a) it is $35t_{\text{dyn}}/\hat{\sigma}_{DM}$. As expected the evolution seems to occur on the relaxation time scale associated with the mean interaction radius $a/2$.

Unlike globular clusters, the $\rho \propto 1/r$ cusped density distributions evolve rapidly, and core collapse occurs after only 5 half-mass relaxation times (Quinlan 1996). The 2-body relaxation results will significantly overestimate the actual core collapse time scale because the SIDM scattering is not diffusive. A particle undergoes one scattering with $\Delta v \sim v$ rather than slowly diffusing in energy due to many small scatterings. Crudely, we expect the system to form a constant density core of size $\simeq a/2$ on the time scale t_{rc} and core collapse faster than the 2-body relaxation prediction of 5 half-mass relaxation times. After core collapse, the system will have a steeper $\rho \propto 1/r^2$ cusp. This is just the behavior we see in the simulations, as we now describe.

4.2. Core formation

We first examined the formation of a core and the alteration of rotation curves as a function of the dimensionless cross section $\hat{\sigma}_{DM}$. Fig. 1 shows the density distributions at $t \simeq t_{\text{dyn}}$ for all five simulations. The scattering clearly produces a constant density core, while the simulation without any scattering roughly maintains the input density cusp. However, even after such a short time interval, the $\hat{\sigma}_{DM} = 10$ simulation has begun its core collapse phase and has a higher central density than any of the other SIDM cases. Our results are very similar to those of Burkert (2000), but the higher scattering rates found with the better approximation to the scattering rate integral mean that we obtain the same evolution with approximately 1/3 the SIDM cross section.

We non-parametrically estimate the core radius by the point where the density drops to 1/4 the central density. The central density is found by finding the region over which the Kolmogorov-Smirnov test provides a reasonable likelihood that the particle distribution is consistent with a constant density. This tends to provide us with an upper limit to the core radius, with an accuracy that is limited primarily by the finite particle number at very small radii. Fig. 2 shows the evolution of the core radius with time and the central density with core relaxation time t_{rc} . For comparison, the core radius due to the finite particle number and numerical relaxation effects starts on the force smoothing scale ($0.05a$) and slowly evolves to $0.1a$, which represents a negligible systematic error for the much larger core radii created by the SIDM (recall our estimate of the core radius is in fact an upper limit). We also find that the evolution of the $\hat{\sigma}_{DM} = 1$ system with 8×10^5 particles is identical to the standard simulation with 10^5 particles (see Fig. 2a).

The system evolution is remarkably rapid, with a very narrow window between the formation of a significant core radius and its recollapse. The maximum core size is approximately $0.4a$ and it forms on the core relaxation time scale $t \simeq t_{rc} = 1.7t_{\text{dyn}}/\hat{\sigma}_{DM}$. Almost immediately af-

ter reaching its maximum size the core begins to collapse again, leaving a brief window where the dark matter shows a large core radius. Although the formation of the core seems to be nearly independent of $\hat{\sigma}_{DM}$ when we scale the time by the core relaxation time scale, the subsequent core collapse phase is not. The rate of recollapse in units of t_{rc} appears to accelerate as the cross section decreases (see Fig. 2b). Empirically we find the evolution of the central density after the reaching the maximum core radius is self-similar if we scale the time in units of $t_{rc}\hat{\sigma}_{DM}^{1/2} \propto \hat{\sigma}_{DM}^{-1/2}$ (see Fig. 2c), which is a different scaling from that for normal 2-body relaxation where the collapse depends only on the relaxation time ($\propto \hat{\sigma}_{DM}^{-1}$). We hypothesize that the difference arises because the scattering is not a diffusive process. In each scattering $\Delta v \sim v$ and particles escape the core in a single scattering, leading to faster evolution.

4.3. Adiabatic Contraction

Very careful tuning of the SIDM cross section and ages might allow dwarf galaxies to have softened cores today without undergoing core collapse. However, we must examine the effects of the baryons on the dark matter profile to estimate the appropriate cross section, as the cooling baryons will adiabatically compress the SIDM dark matter and significantly modify the evolution of the system. The adiabatic compression both raises the scattering rates and reduces the relaxation time scales in three ways. First, by raising the densities and reducing the dynamical time scale, the relaxation time drops. Very crudely, if we compress the dark matter by a factor of f , the scattering rate jumps by a factor of $f^{7/2}$, producing a corresponding reduction in the relaxation time. A second, more subtle factor is the difference in how density cusps and density distributions with cores are adiabatically compressed. Standard adiabatic compression models for a $1/r$

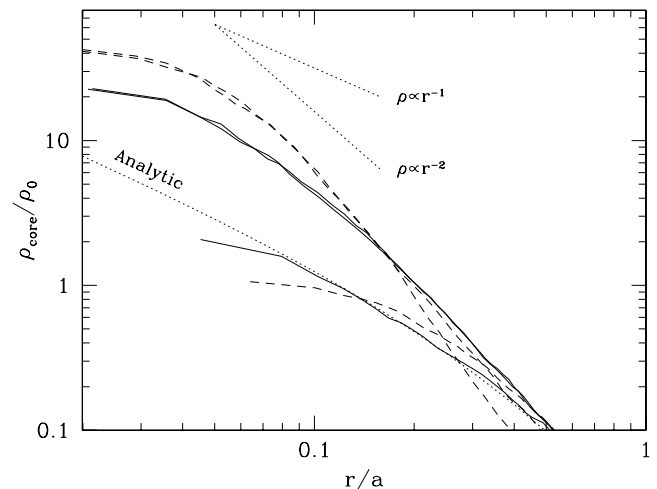


FIG. 3.— The combined effects of SIDM and adiabatic compression. The SIDM cross section is $\hat{\sigma} = 0$ (solid) or 1 (dashed) and the adiabatically compressed curves include the baryonic contribution (Eq. 12). Curves of increasing central density are just before the compression ($t = t_{\text{dyn}}$), just after the compression ($t = 3t_{\text{dyn}}$) and some time after compression ($t = 4.0t_{\text{dyn}}$). The force smoothing scale is $0.01a$.

density cusp will maintain a $1/r$ density cusp after the compression (see Quinlan, Hernquist & Sigurdsson 1995) while the compression of a density distribution with a finite core radius produces a steeper ($1/r^{3/2}$ to $1/r^{9/4}$) cusp depending on the distribution function (Young 1980). Thus, if the SIDM produces a core radius before the adiabatic compression phase, the adiabatic compression produces a steeper than normal central density cusp. In 2-body relaxation, steep cusps evolve more rapidly than shallow cusps, and Quinlan (1996) found that where a $1/r$ density cusp reaches core collapse in 5 half-mass relaxation times, a $1/r^2$ density cusp reaches core collapse in 1 half-mass relaxation time. Hence the steeper central cusp created by adiabatic compression of the SIDM core further accelerates the ultimate evolution of the system to a central $1/r^2$ density cusp. Third, the existence of the baryonic matter provides a component of the gravitational potential whose evolution is not driven by scattering.

We investigate this with a single, somewhat contrived experiment. We put 20% of the mass of the profile in an analytic Hernquist potential with a corresponding reduction in the masses of the dark matter particles. We modeled the adiabatic compression by running the system for t_{dyn} , and then slowly changing the external potential to

$$\phi(r) = \frac{-GM_b}{\sqrt{r^2 + a_d^2}} \quad (12)$$

between t_{dyn} and $2t_{\text{dyn}}$, finally fixing the external potential for the further evolution. We used $M_b = 0.2M_T$, $a_d = 0.1a$, and reduced the force smoothing to $0.01a$. The final external potential was chosen to have the same circular velocity profile as a Kuzmin disk (Binney & Tremaine 1987), and underestimates the amount of compression compared to the standard approximation (Blumenthal et al. 1986). It corresponds to a baryonic density

$$\rho(r) = \frac{3M_b}{4\pi} \frac{a_d^2}{(r^2 + a_d^2)^{5/2}}. \quad (13)$$

At the end of the compression phase, the central dark matter density has risen by a factor of ~ 10 . We ran the compression sequence with either $\hat{\sigma}_{DM} = 0$ or 1.

Fig. 3 shows the dark matter density and rotation curve profiles of the adiabatically compressed systems both at the end of the compression phase ($3t_{\text{dyn}}$) and the end of the experiment ($4t_{\text{dyn}}$). At the start of the compression, the scattering has begun to establish the typical SIDM core structure. The adiabatic compression then produces significantly different central density profiles. The no scattering simulation maintains a roughly $\rho \propto 1/r$ profile shifted upwards in density, while the $\hat{\sigma}_{DM} = 1$ simulation has formed a steeper, nearly $\rho \propto 1/r^2$ profile with a *higher* central dark matter density than if there had been no scattering, just as we expected from the differences in how the two profiles would be adiabatically compressed. In the subsequent evolution, the no scattering simulation maintains a stable profile while the $\hat{\sigma}_{DM} = 1$ simulation has a rising central density. The system appears to proceed directly into the core-collapse phase of its evolution despite the fixed baryonic potential.

4.4. Spherical Collapse

Our previous experiments assumed that no significant scattering occurred during the initial collapse of the dark matter halo so that the initial conditions contained a $\rho \propto 1/r$ density cusp. We also considered how the formation of the halo is altered in the SIDM model by considering the very simple case of the collapse of a top-hat overdensity with vacuum boundary conditions both with and without the DM scattering. These simulations are meant only to illustrate the primary effects of DM scattering on collapsing perturbations, and not as realistic models of the formation of galaxies or clusters in a cosmological context.

We generated a 10^5 particle uniform density sphere with velocity dispersion 1% of the virial velocity and allowed it to collapse. Without particle scattering the collapse formed a profile akin to the Hernquist profiles of the previous sections, with some of the particles being ejected from the system. By fitting a Hernquist profile to the resulting system we identified the scattering rate appropriate to $\hat{\sigma}_{DM} \simeq 1$ and re-ran the simulation from the same initial conditions including scattering.

The simulations indicate that the final equilibrium profile is similar with and without scattering, however at fixed dynamical time the scattering run always has a higher central density. We postulate that the scattering provides a mechanism, similar to dissipation, which allows the system to attain higher phase space densities than are possible in a purely collisionless/dissipationless collapse.

5. CONCLUSIONS

We combined an N-body code with a Monte Carlo model of scattering to examine the effects of self-interacting dark matter (SIDM) on the properties of dark matter halos. Our models form a one parameter family with “standard” CDM as a limiting case.

We first examined the time evolution of Hernquist models with $1/r$ central density cusps in the presence of SIDM. Our simulations are similar to those of Burkert (2000), but use a better approximation to the scattering integrals. The models form a constant density core with a radius $\sim 0.4a$ on the core radius relaxation time scale $t_{rc} = 1.7t_{\text{dyn}}/\hat{\sigma}_{DM}$, where the SIDM cross section per unit mass is $\hat{\sigma}_{DM} = \sigma_{DM}M_T/a^2$. The initial growth of the core radius is very rapid because the relaxation time is much shorter in the inner regions (see Quinlan 1996). Shortly after reaching this maximum core size the core begins to shrink. We find that the recollapse proceeds on a faster time scale than expected from 2-body relaxation. The central density evolution evolves on time scales of $t_{rc}\hat{\sigma}_{DM}^{1/2} \propto \hat{\sigma}_{DM}^{-1/2}$ rather than $t_{rc} \propto \hat{\sigma}_{DM}^{-1}$, probably because SIDM is not a diffusive process when the mean free paths are large. Thus, the dark matter briefly has a large, finite core radius which could be fine tuned to address the problem of dwarf galaxy rotation curves at the expense of predicting core collapsed dark matter halos with $\rho \propto 1/r^2$ cusps in most other galaxies. In particular, it is probably impossible to use SIDM to eliminate the dark matter cusps in the dwarf galaxies while preserving them in the low surface brightness galaxies.

Even with SIDM, however, we must also consider the role of the baryons in modifying the structure of the dark matter halo. In particular, as the baryons cool and form

a disk they adiabatically compress the dark matter (Blumenthal et al. 1986; Dubinski 1994). The adiabatic compression raises the central dark matter density, increases the SIDM scattering rate, and reduces the time scale for core collapse. Moreover, adiabatic compression of a density profile with a finite core radius produces a steep central density cusp (Young 1980) which relaxes to form a $\rho \propto 1/r^2$ density cusp even faster than the shallower $\rho \propto 1/r$ cusp we considered initially (Quinlan 1996). As a result, the development of a core radius due to the SIDM scattering is first reversed by the compression, and then core collapse begins on a far shorter time scale. Such a further acceleration of the time scale for producing a final density distribution with a steep $\rho \propto 1/r^2$ density cusp will make it even harder for SIDM to maintain a core radius in the dark matter profile for periods comparable to the presumed lifetimes of dwarf galaxies.

All of the above simulations supposed that the halo collapsed and virialized before scattering became important, which is appropriate to “low” scattering rates. Finally, we considered the effects of SIDM on the collapse of cold top-hat perturbations with $\hat{\sigma}$ large enough that scattering and virialization could occur at the same time. We found that the scattering allowed higher phase space densities at fixed dynamical time than could be found in the collisionless systems.

It thus appears as though SIDM exacerbates rather than solves the “central density cusp problem”. Turning this around we can say that astrophysics almost certainly requires SIDM cross sections small enough to avoid significant scattering over the age of the universe for all galaxies, or mean free paths $\gtrsim 1$ Mpc.

We would like to acknowledge useful conversations with A. Burkert and L. Hernquist. M.W. thanks J. Bagla and V. Springel for numerous helpful conversations on N-body codes. M.W. was supported by NSF-9802362, and C.S.K. was supported by the Smithsonian Institution.

APPENDIX

TREE N-BODY CODE

We have used a new implementation of a *Tree* code to evolve our dark matter halo. Since this code is new we briefly describe it here, and also explain how we generated the initial conditions.

The basic algorithm is described in Barnes & Hut (1986). Space is partitioned into an oct-tree structure by bisection in the three spatial dimensions. Starting at the root node, which is the entire volume of the simulation, the tree descends until each node contains at most one particle. The force on any given particle from all of the other particles is computed by a tree walk. The speed-up over direct summation is obtained by imposing an opening criterion during the tree walk. For cells sufficiently far from the particle in question, the entire mass distribution within that cell is approximated by a point at the center of mass of the cell and with mass equal to the sum of the particle masses within the daughters of that cell.

Though the code does not require it, we have used equal mass particles throughout. The size of the computational

box grows so as to always encompass all of the particles. Rather than a Plummer potential we use a spline softened force (Monaghan & Lattanzio 1985; Hernquist & Katz 1989; Springel, Yoshida & White 2000). For most of the runs we use $h = 0.05a$ (the force was therefore exactly $1/r^2$ beyond h), but for the adiabatic compression runs we lower this to $0.01a$. Very roughly this corresponds to a Plummer law smoothing $\epsilon \simeq h/3$, although a Plummer law gives 1% force accuracy only beyond 10ϵ .

With 10^5 particles it is finite particle numbers which limit our resolution, *not* force accuracy. For profiles with almost any central cusp, the relaxation time is less than $10t_{\text{dyn}}$ for radii $r < 0.05a$ (Quinlan 1996). Our numerical results with differing particle numbers and force accuracies support the scalings in Fig. 2 of Quinlan (1996). Only for the adiabatic compression runs, where more particles are concentrated at small radius and there is a stable external potential, do we gain by lowering h .

The time integration is done with a second order leap-frog method. The time step is chosen to be the smaller of $0.5\sqrt{h/a_{\text{max}}}$, where a_{max} is the maximum acceleration on the particle, or $2h/v$ where v is the particle velocity. We have shown that this time step accurately integrates binary orbits, and in combination with the opening criterion described below conserves total energy to much better than a percent over 5 dynamical times, except during the core collapse phase where the error rises to a few percent.

Finally for the tree walk we do not simply use the geometrical criterion advocated by Barnes & Hut. Rather we have augmented it with a modification of the method described in Springel et al. (2000). Starting with the known accelerations from the last time step we descend the tree. We open an internal node if the partial acceleration from the quadrupole moment of that node exceeds α times the old acceleration, where α is a tolerance parameter. Specifically if ℓ is the size of a cell containing mass M whose center of mass is a distance r from the particle in question, we open the node if

$$M\ell^2 > \alpha |\vec{a}_{\text{old}}| r^4 \quad . \quad (\text{A1})$$

This ensures that the relative force accuracy is $\mathcal{O}(\alpha)$ while the resulting tree walk is significantly faster (Springel et al. 2000). The tree walk is also used to define the neighbor list for the density and scattering calculations. To ensure that all nearby cells are opened so the neighbor list is “complete” we augment the opening criterion to additionally require that $\ell < \theta r$ for cells closer than a . This provides a good estimate of the density except in the lowest density regions where the scattering probability is anyway small. Throughout we have used $\alpha = 2\%$ and $\theta = 0.4$, which for a Hernquist profile results in a 90th percentile relative force error of 5×10^{-3} , i.e. 90% of the particles have force errors less than this.

We set up our initial conditions as a Hernquist (1990) profile

$$\rho_H(r) = \frac{M_{\text{halo}}}{2\pi} \frac{a}{r} \frac{1}{(r+a)^3} \quad (\text{A2})$$

where a is the scale-length. First we choose the position of a particle with a radial probability distribution proportional to $r^2\rho(r)$ and an isotropic \hat{r} . We impose an upper radial distance of $r_{\text{max}} = 50a$ at which point the density is $\sim 10^{-5}$ of the density at $r = a$. Given the posi-

tion we then calculate the magnitude of the velocity from the known distribution function $f(E)$ for this model using an acceptance-rejection method and again distribute \hat{v} isotropically. This procedure is iterated $N_p/2 = 5 \times 10^4$ times. Each particle and a reflected counterpart at $-\vec{r}$ with velocity $-\vec{v}$ is added to the list to obtain a realization of the halo with N_p particles. The use of ‘reflected’ initial conditions ensures that the center of mass position and velocity of the halo are both initially zero.

REFERENCES

- Barnes J., Hut P., 1986, *Nature*, 324, 446
 Bento, M.C., Bertolami, O., Rosenfeld, R., & Teodoro, L., 2000, preprint [astro-ph/0003350]
 Binney J., Gerhard, O., & Silk, J., 2000, preprint [astro-ph/0003199]
 Binney J., Tremaine S., 1987, “Galactic Dynamics”, Princeton UP
 Blumenthal G.R., Faber S.M., Flores R., Primack J.R., 1986, *ApJ*, 301, 27
 Bullock J., Kravstov A.V., Weinberg D.H., 2000, preprint [astro-ph/0002214]
 Burkert A., 2000, preprint [astro-ph/0002409]
 Carlson E.D., Machacek M.E., Hall L.J., 1992, *ApJ*, 398, 43
 Dubinski J., 1994, *ApJ*, 431, 617
 Faber, S.M., Tremaine, S., Ajhar, E.A., Byun, Y.-I., Dressler, A., Gebhardt, K., Grillmair, C., Kormendy, J., Lauer, T.R., & Richstone, D., 1997, *AJ*, 114, 1771
 Firmani C., et al., 2000, preprint [astro-ph/0002376]
 Flores R., Primack J.R., 1994, *ApJ*, 427, L1
 Gelato, S. & Sommer-Larsen, J., 1999, *MNRAS*, 303, 321
 Hannestad S., 2000, preprint [astro-ph/9912558]
 Hannestad S., Scherrer R.J., 2000, preprint [astro-ph/0003046]
 Hernquist L., 1990, *ApJ*, 356, 359
 Hernquist L., Katz N., 1989, *ApJS*, 70, 419
 Hernquist, L. & Weinberg, M.D., 1992, *ApJ*, 400, 80
 Hogan C.J., Dalcanton J.J., 2000, preprint [astro-ph/0002330]
 Hozumi, S., Burkert, A. & Fujiwara, T., 2000, *MNRAS*, 311, 377
 Huss A, Jain B., Steinmetz M., 1999, *ApJ*, 517, 64
 Klypin A., Kravstov A.V., Valenzuela O., Prada F., 1999, *ApJ*, 522, 82
 Kravstov A.V., et al., 1998, *ApJ*, 502, 48
 Kull A., 1999, *ApJ*, 516, L5
 de Laix A.A., Scherrer R.J., Schaeffer R.K., 1995, *ApJ*, 452, 495
 MacLow, M.-M., & Ferrara, A., 1999, *ApJ*, 513, 142
 Mo H.J., Mao S., 2000, preprint [astro-ph/0002451]
 Monaghan J.J., Lattanzio J.C., 1985, *Astr Ap*, 149, 135
 Moore B., 1994, *Nature*, 370, 629 [astro-ph/9402009]
 Moore B., Governato F., Quinn T., Stadel J. Lake G., 1998, *ApJ*, 499, L5
 Moore B., Quinn T., Governato F., Stadel J., Lake G., 2000a, preprint [astro-ph/9903164]
 Moore B., et al., 1999, *ApJ*, 524, L19
 Moore B., et al., 2000b, preprint [astro-ph/0002308]
 Navarro J., Eke, V.R., & Frenk C.S., 1996, *MNRAS*, 283, L72
 Navarro J., Frenk C., White S.D.M., 1997, *ApJ*, 490, 493
 Ostriker J.P., 2000, preprint [astro-ph/9912548]
 Quinlan G.D., Hernquist, L., & Sigurdsson, S., 1995, *ApJ*, 440, 554
 Quinlan G.D., 1996, *NewA*, 1, 255
 Spergel D.N., Steinhardt P.J., 2000, preprint [astro-ph/9909386]
 Springel V., Yoshida N., White S.D.M., 2000, preprint [astro-ph/0003162]
 Syer D., White S.D.M., 1998, *MNRAS*, 293, 337
 van den Bosch F.C., Robertson B.E., Dalcanton J.J., de Blok W.J.G., 2000, *AJ*, in press [astro-ph/9911372]
 Yoshida N., Springel V., White S.D.M., Tormen G., 2000, preprint [astro-ph/0002362]
 Young, P., 1980, *ApJ*, 242, 1232